Carderock Division
Naval Surface Warfare Center
W. Bethesda, MD 20817-5700

NSWCCD-72--TR-2003/099 September 2003

Signatures Directorate
Research and Development Report

Leading Edge Noise from Thick Foils in Turbulent Flows

By:
Jonathan Gershfeld, NSWCCD 725

NSWCCD-72--TR- TR-2003/099 September 2003 Leading Edge Noise from Thick Foils in Turbulent Flows

REPORT DOCUMENTATION PAGE

Form Approved
OMB No. 0704-0188

1. AGENCY USE ONLY (*Leave Blank*)	2. REPORT DATE	3. REPORT TYPE AND DATES COVERED	
	30 September 2003	Final	04/01/02 - 06/30/03

4. TITLE AND SUBTITLE
Leading Edge Noise from Thick Foils in Turbulent Flows

5. FUNDING NUMBERS

6. AUTHOR(S)
Jonathan Gershfeld

7. PERFORMING ORGANIZATION NAME(S) AND ADDRESS(ES)
Naval Surface Warfare Center
Carderock Division
9500 MacArthur Boulevard
West Bethesda, MD 20817-5700

8. PERFORMING ORGANIZATION REPORT NUMBER
NSWCCD-72-TR-2003/099

9. SPONSORING/MONITORING AGENCY NAME(S) AND ADDRESS(ES)
Commander Naval Sea Systems Command
SUB-RT
1333 Isaac Hull Avenue SE
Washington Navy Yard, DC 20376

10. SPONSORING/MONITORING AGENCY REPORT NUMBER

11. SUPPLEMENTARY NOTES

12a. DISTRIBUTION/AVAILABILITY STATEMENT
Approved for public release; Distribution is unlimited.

12b. DISTRIBUTION CODE

13. ABSTRACT (*Maximum 200 words*)

The prediction of dipole sound from the diffraction of turbulence by the leading edge of a thick foil is made with the Kirchhoff integral for rigid surface scattering of the stagnation enthalpy. The incident field is determined from a volume integral and the rigid plane Green function using an equivalent form of Howe's (1975) acoustic analogy that is derived in terms of the mean free stream velocity and the fluctuating up-wash velocity found in Sears'(1941) analysis. A comparison of the measured and the predicted dipole sound made with the foil geometry and measured turbulence statistics from Paterson and Amiet (1976) shows good agreement. The thickness effect is incorporated in the governing Green function for the foil [Howe (1998a, 2001a)] and serves to exponentially attenuate the dipole sound pressure spectrum by the product of the convection wave number and half the maximum section thickness. The dipole sound from a foil cutting through a mean shear layer is then calculated using an acoustic analogy where the source has retained the mean shear term. The ratio of the dipole sound of the mean shear source to the source without mean shear from the earlier calculation is determined to be proportional to the ratio of the mean shear to the frequency of the sources. Estimates of the dipole sound with and without the mean shear source are made for Olsen and Wagner's (1982) experiment.

14. SUBJECT TERMS	15. NUMBER OF PAGES
	48
	16. PRICE CODE

17. SECURITY CLASSIFICATION OF REPORT	18. SECURITY CLASSIFICATION OF THIS PAGE	19. SECURITY CLASSIFICATION OF ABSTRACT	20. LIMITATION OF ABSTRACT
UNCLASSIFIED	UNCLASSIFIED	UNCLASSIFIED	SAR

CONTENTS

FIGURES

ABSTRACT

The prediction of dipole sound from the diffraction of turbulence by the leading edge of a thick foil is made with the Kirchhoff integral for rigid surface scattering of the stagnation enthalpy. The incident field is determined from a volume integral and the rigid plane Green function using an equivalent form of Howe's (1975) acoustic analogy that is derived in terms of the mean free stream velocity and the fluctuating up-wash velocity found in Sears'(1941) analysis. A comparison of the measured and the predicted dipole sound made with the foil geometry and measured turbulence statistics from Paterson and Amiet (1976) shows good agreement. The thickness effect is incorporated in the governing Green function for the foil [Howe (1998a, 2001a)] and serves to exponentially attenuate the dipole sound pressure spectrum by the product of the convection wave number and half the maximum section thickness. The dipole sound from a foil cutting through a mean shear layer is then calculated using an acoustic analogy where the source has retained the mean shear term. The ratio of the dipole sound of the mean shear source to the source without mean shear from the earlier calculation is determined to be proportional to the ratio of the mean shear to the frequency of the sources. Estimates of the dipole sound with and without the mean shear source are made for Olsen and Wagner's (1982) experiment.

ADMINISTRATIVE INFORMATION

This work was funded by the 93R Advanced Propulsors Program, Task 1 Blade Shaping. The Document/Sponsor no. was N0002402WR10228, the Appropriation was RDT&E, the Program Element no. was 0603561N, and the Project Task no. was S2033.

1. Introduction

An airfoil in a turbulent flow generates a net distribution of acoustic dipoles primarily at the leading and trailing edges. In these regions, the dipole surface normal stresses induced by the turbulence are not canceled by their images due to the surface curvature [Powell (1960), Meecham (1965)]. Sears (1941) modeled the incompressible unsteady lifting force associated with the dipoles by representing the foil as an acoustically compact two-dimensional strip. His analysis included a trailing edge Kutta condition and showed for fluctuating velocities much smaller than the free stream velocity that the unsteady lifting force was proportional to the product of the mean free stream velocity and the fluctuating "up-wash" velocity. The application of the Kutta condition essentially removed this edge's contribution to the incompressible part of the total unsteady lift for reduced frequencies greater than one (based on the chord length) [Howe (2001b)].

When the airfoil chord length is acoustically non-compact, the dipole sound produced from the diffraction of the turbulence by either the leading or trailing edge is subsequently "back-scattered" by the opposite edge of the foil. Landhal (1961), Adamczyk (1974), Amiet (1975), and Martinez and Widnall (1980) accounted for the back scattering by the trailing edge of the leading edge dipole sound for a surface without thickness. Roger, Moreau and Wang (2002) extended Amiet's (1975) solution with a second scattering correction term for application to a trailing edge noise problem. Howe (2001a) constructed a Green function to account for the multiple back scattering by both edges. The Green function also included the dependence of the shape of the edge for the diffraction of the incident turbulence [Howe (1975)]. In practice, the use of a Green function to predict the dipole sound produced by the diffraction of a turbulent flow requires that the spatial distribution of the incident sources be prescribed and remain frozen within the diffraction zone. This "rapid distortion" approximation attributes the diffraction to the Green function and does not account for any interaction between the incident sources and their images [Howe (1999)]. This approximation is satisfactory as long as the turbulence fluctuations are less than 10% of the free stream velocity [Grace (2001)].

The acoustic analogy of Howe (1975) has been utilized with a shape dependent Green function to estimate the dipole sound from the diffraction of the sources within turbulent boundary layers by trailing edges of various contours [Howe (1998a and b), (1988), (2000)].

Calculations of the shape dependence of the unsteady lift for turbulence encountering the leading edge have been restricted to numerical models with idealized representations of the flow acoustic source. The spatial domain formulation of the blade vortex interaction (BVI) models of Martinez and Rudzynsky (1997) and Grace (2001) predict a reduction in unsteady lift with increasing frequency for a thick foil relative to a foil without thickness. These trends agree with the leading edge dipole sound measurements made by Olsen and Wagner (1982) with airfoils of varying thickness. The BVI calculations are also substantiated by the difference between the measured dipole sound spectra from a NACA 0012 airfoil and the sound spectra predicted by a zero thickness theory [Paterson and Amiet (1976, 1977)] as illustrated in Fig. 1.1. Paterson and Amiet ascribed the discrepancy between their theory and data to the thickness of the foil for convection wavelengths of the incident turbulence that were smaller than the foil thickness. Grace (2001) showed that calculations performed in the wave number domain of the unsteady lift response of thick foils to "gusts" incident to the leading edge do not capture the observed thickness dependence.

The current work uses an acoustic analogy and a shape dependent Green function to predict the lifting dipole sound from the leading edge diffraction of homogeneous turbulence by a thick, symmetric foil at a zero angle of attack to the mean flow. The foil thickness, h, is restricted to being acoustically compact, ($hk_o<<1$) while the chord length, c, can be greater than an acoustic wavelength, $\lambda = 2\pi/ k_o$, ($ck_o>1$).

In Section 2, the portion of the Howe (1975) aero-acoustic source that generates the lifting component of the dipole sound is expressed in terms of the mean free stream velocity and the fluctuating up-wash velocity that also arises in Sears' (1941) analysis. The source is tailored to be linear in fluctuating variables, without mean shear [Blake (1986), Howe (1989)] and spatially homogeneous. The near field of the quadrupole radiation on a rigid plane is then obtained from the volume integral of this source with the appropriate Green function.

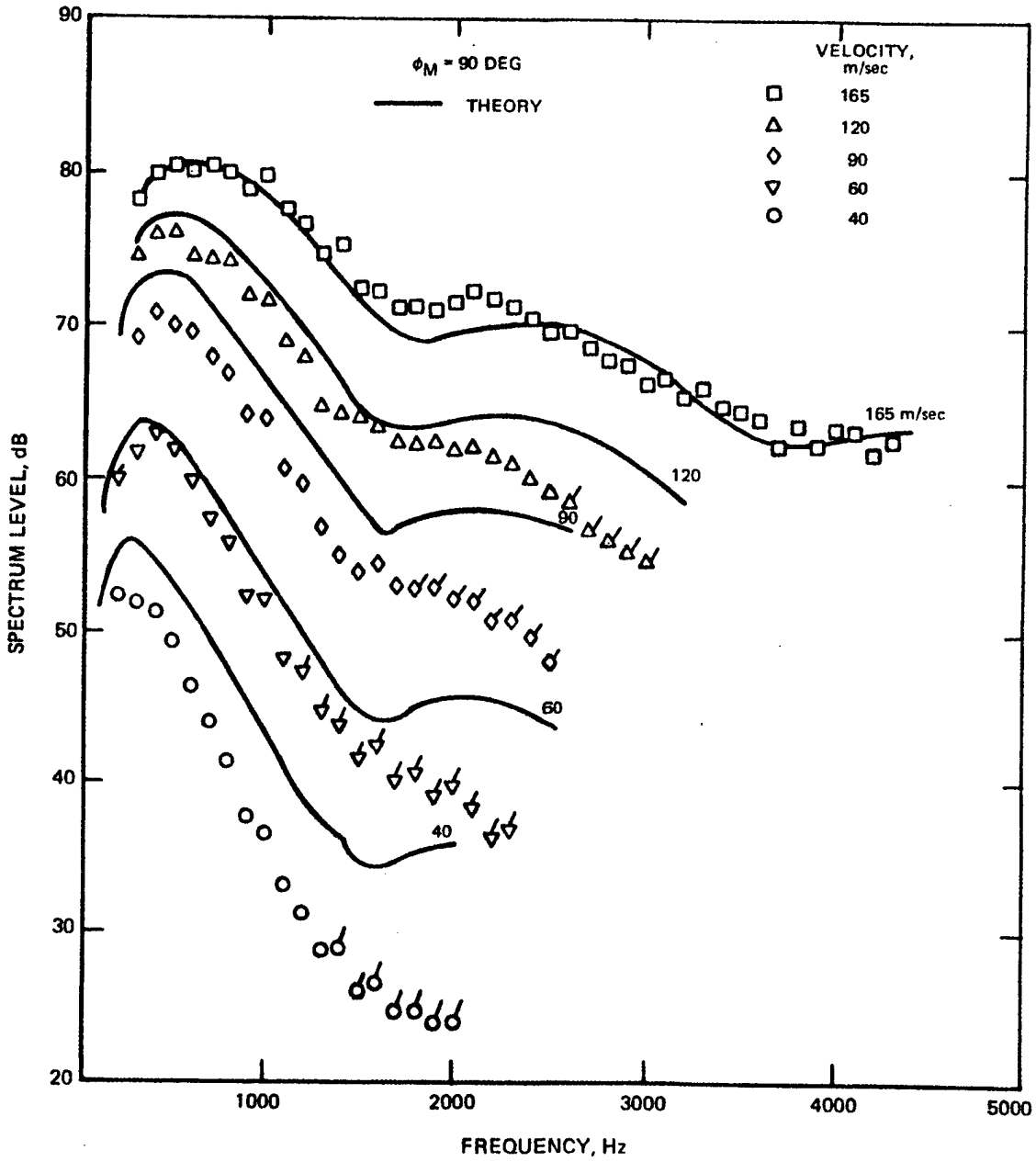

Figure 1.1 A comparison of the measured (points) and predicted far-field dipole sound (lines). Originally published in "Noise and Surface Pressure Response of an Airfoil to Incident Turbulence," by R. W. Paterson and R. K. Amiet, Journal of Aircraft, Vol. 14, No. 8, pp. 729-736, Fig. 4.

In Section 3, the leading edge lifting dipole sound produced by a foil is modeled by the Kirchhoff integral for rigid surface diffraction of the stagnation enthalpy. The Green function incorporates the effect of the foil thickness [Howe (1998a)] and the acoustic non-compactness of the airfoil's chord length [Howe (2001a)]. The incident surface stagnation enthalpy is expressed in terms of the mean velocity and the fluctuating up-wash velocity spectrum obtained from Section 2. This formula, along with the measurements of the incident flow turbulence reported by Paterson and Amiet (1976, 1977), are used to predict the measured dipole sound for a NACA0012 airfoil (h/c=0.12) and the corresponding zero thickness theory (h/c=0) for a variety of reported flow speeds.

In Section 4, the acoustic source is tailored to be linear with respect to fluctuating terms and to contain the mean shear [Kraichnan (1956), Chase (1980), Blake (1986)]. This source is specified to be homogeneous, and the imposed surface pressure spectrum from the quadrupole radiation on a rigid plane surface is obtained. The calculated surface pressure spectrum for the mean shear flow, when combined with the results of Section 2, yield a prediction formula for the leading edge lifting dipole sound of a thick, acoustically non-compact foil cutting through a shear layer. Estimates of the measured leading edge dipole sound by Olsen and Wagner (1982) are made for incident sources with and without the mean shear term. These estimates establish the frequency below which the mean shear source dominates the source without mean shear.

2. Wall Stagnation Enthalpy Spectrum from Homogeneous Turbulence Without Mean Shear

The stagnation enthalpy spectrum, B, imposed on a rigid plane (y_1, $y_2 = 0$, y_3) will be calculated from the quadrupole radiation of a spatially homogeneous turbulence field as illustrated in Fig. 2.1. The turbulent flow is specified to have no mean shear so that the resultant wall stagnation enthalpy spectrum will serve as the incident field that will be used in Section 3 to calculate the leading edge noise from homogeneous turbulence in the absence of mean shear. The radiating stagnation enthalpy, **B**, is described by the acoustic analogy of Howe (1975) for vortex sound

$$\nabla^2 \mathbf{B} - \frac{\partial^2 \mathbf{B}}{\partial t^2} = -\nabla \cdot (\boldsymbol{\Omega} \times \mathbf{U}) \,, \tag{2.1}$$

where $\boldsymbol{\Omega}$ and $\mathbf{U}$ represent respectively, the sum of the mean and fluctuating vorticity and velocity. The stagnation enthalpy is expressed in terms of the acoustic pressure, p, the fluid density, ρ, and the fluctuating velocity, u:

$$B = \int dp/\rho + 0.5u^2 \,. \tag{2.2}$$

The component of the hydro-acoustic source that contributes to the lifting dipoles with axes aligned normal to the free streamlines [Blake (1986), Howe (1989)] shall be used to model the incident source

$$\nabla \cdot (\Omega' \times U') = \frac{\partial}{\partial y_2} (\Omega'_3 \times U_1)(y,t) \,. \tag{2.3}$$

The primed (') variables are in the time domain, and the subscripts 1, 2 and 3 denote respectively the streamwise, spanwise, and surface normal directions. The source is linear with respect to the fluctuating terms, and only the spanwise vorticity, Ω_3, contains the fluctuating

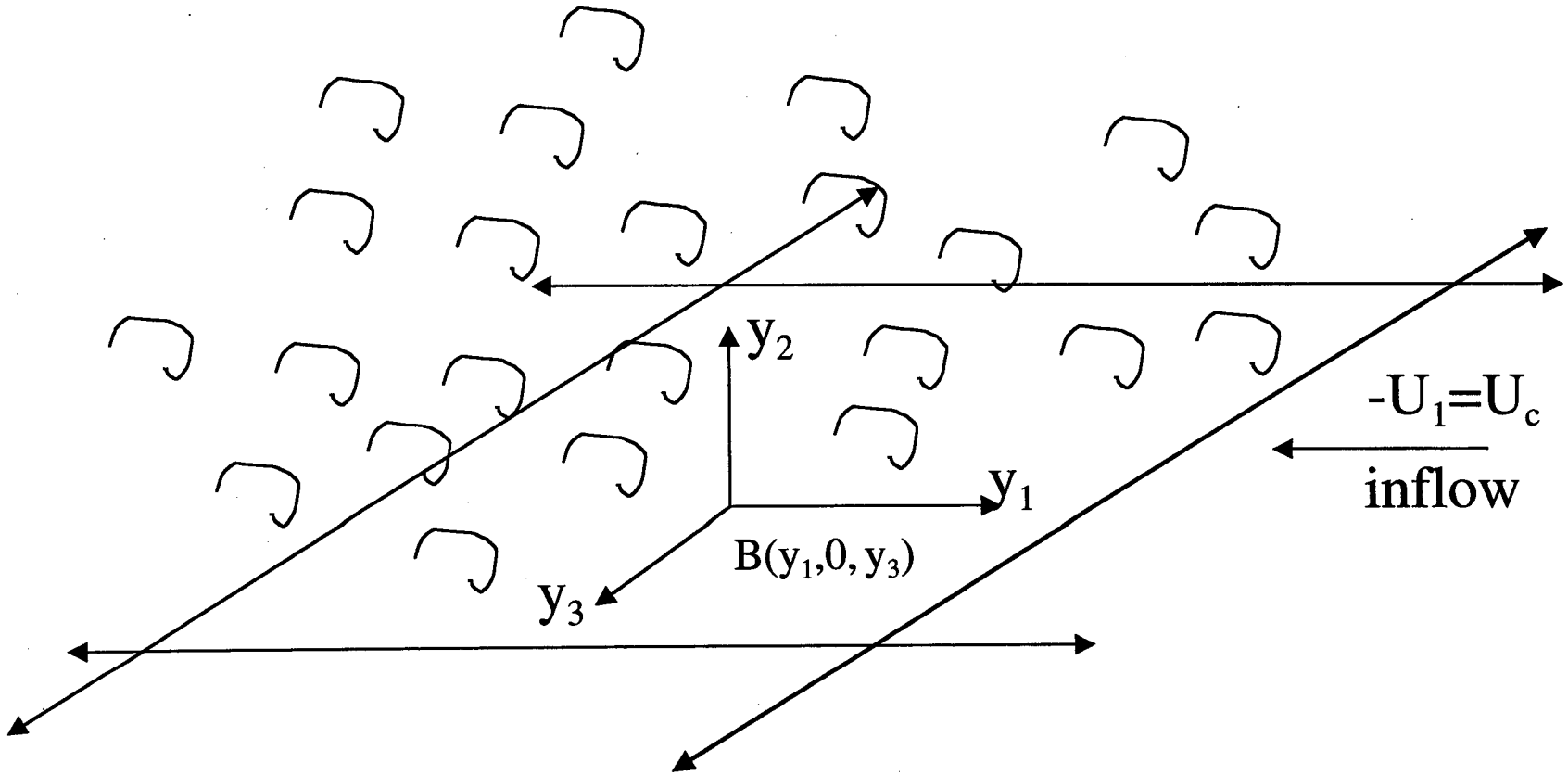

Figure 2.1 Homogeneous turbulence over a rigid plane and imposed wall stagnation enthalpy, $B(y_1, 0, y_3)$.

components of the source. The subsequent planar wave number spectrum of the near field radiation is given by Blake (1986)

$$B(k,\omega)=\frac{1}{(2\pi)^2}\iiint_V dV(y)\frac{\partial}{\partial y_2}(\Omega_3\times U_1)(y,\omega)\iint_S d^2x_{1,3}\frac{e^{-ik_{1,3}\cdot x_{1,3}+ik_o r}}{r}, \tag{2.4}$$

where the unprimed variables have been Fourier transformed from time to frequency and $k_{1,3}=(k_1, k_3)$, $x_{1,3}=(x_1, x_3)$, $d^2x_{1,3}=dx_1dx_3$. When the in-plane Fourier transform of the Green function

$$\frac{1}{2\pi}\iint_{-\infty}^{+\infty}\frac{e^{ik_0 r}}{r}e^{-ik_{1,3}\cdot x_{1,3}}d^2x_{1,3}=i\frac{e^{iy_2\gamma(k)}}{\gamma(k)}e^{-ik_{1,3}\cdot y_{1,3}} \tag{2.5}$$

is substituted into Eq. (2.4), the stagnation enthalpy wave number spectrum becomes

$$B(k,\omega)=\frac{1}{(2\pi)^2}\iiint_V dV(y)\frac{\partial}{\partial y_2}(\Omega_3\times U_1)i\frac{e^{iy_2\gamma(k)}}{\gamma(k)}e^{-ik_{1,3}\cdot y_{1,3}}, \tag{2.6}$$

where

$$\gamma(k)=\sqrt{k_o^2-k_1^2-k_3^2}$$

and $k_o=\omega/c_o$, is the acoustic wave number. Rearranging the terms of Eq. (2.6),

$$B(k,\omega)=\frac{1}{(2\pi)^2}\iiint_V dy_2d^2y_{1,3}e^{-ik_{1,3}\cdot y_{1,3}}\frac{\partial}{\partial y_2}(\Omega_3\times U_1)(y_1,y_2,y_3,\omega)i\frac{e^{iy_2\gamma(k)}}{\gamma(k)} \tag{2.7}$$

while taking the Fourier transform of the source variables with respect to the in-plane coordinates (denoted by the over bar):

$$\overline{(\Omega_3 U_1)}(k_{1,3},y_2,\omega)=\iint_{-\infty}^{+\infty} d^2y_{1,3}\frac{1}{(2\pi)^2}e^{-ik_{1,3}\cdot y_{1,3}}(\Omega_3 U_1)(y_1,y_2,y_3,\omega) \tag{2.8}$$

and upon substitution of Eq. (2.8) into Eq. (2.7), in the absence of mean shear, yields the following expression for the wall stagnation enthalpy wave number spectrum:

$$B(k,\omega)=\int_0^{\infty} dy_2 U_1\frac{\partial}{\partial y_2}\overline{(\Omega_3(k_{1,3},y_2,\omega))}\,i\frac{e^{iy_2\gamma(k)}}{\gamma(k)}\,. \tag{2.9}$$

Howe's (1975) acoustic source in Eq. (2.9) can be expressed in terms of the fluctuating up-wash velocity, u_2, and free stream velocity, U_1. The solenoidal velocity wave number spectrum can be expressed in terms of the vorticity wave number spectrum [Howe (1998a]:

$$\begin{aligned}&\hat{u}(k)=ik\times\hat{\Omega}(k)/|k|^2\\&|k|^2=k_1^2+k_2^2+k_3^2\end{aligned}\,. \tag{2.10}$$

The up-wash velocity wave number spectrum becomes:

$$\hat{u}_2(k)=i(k_1\times\hat{\Omega}_3(k))_2/|k|^2\,. \tag{2.11}$$

Rearranging Eq. (2.11),

$$\frac{|k|^2}{k_1}U_1\hat{u}_2(k)=-i(\hat{\Omega}_3(k)\times U_1)_2 \tag{2.12}$$

and taking the inverse Fourier transform Eq. (2.12) with respect to k_2,

$$\int_{-\infty}^{+\infty} dk_2 e^{ik_2y_2}\left(i\frac{|k|^2}{k_1}U_1\hat{u}_2(k_1,k_2,k_3,\omega)\right)=\overline{\Omega_3(k_1,y_2,k_3,\omega)}U_1 \tag{2.13}$$

and then substituting Eq. (2.13) into Eq. (2.9), yields the wall stagnation enthalpy wave number spectrum:

$$B(k,\omega)=\int_0^{\infty} dy_2 \frac{\partial}{\partial y_2}\{\int_{-\infty}^{+\infty} dk_2 e^{ik_2 y_2}(i\frac{|k|^2}{k_1}U_1\hat{u}_2(k_1,k_2,k_3,\omega))\}i\frac{e^{iy_2\gamma(k)}}{\gamma(k)} . \tag{2.14}$$

In the absence of mean shear, Eq. (2.14) becomes:

$$B(k,\omega)=\int_0^{\infty} dy_2 i\frac{e^{iy_2\gamma(k)}}{\gamma(k)}\{\int_{-\infty}^{+\infty} dk_2(ik_2)e^{ik_2 y_2}(i\frac{|k|^2}{k_1}U_1\hat{u}_2(k_1,k_2,k_3,\omega))\} . \tag{2.15}$$

The complex conjugate (*) of the wall stagnation enthalpy,

$$B^*(k',\omega')=\int_0^{\infty} dy'_2(-i)\frac{e^{-iy'_2\gamma^*(k')}}{\gamma^*(k')}\{\int_{-\infty}^{+\infty} dk'_2(-ik'_2)e^{-ik'_2 y'_2}(-i\frac{|k'|^2}{k'_1}U_1\hat{u}_2{}^*(k'_1,k'_2,k'_3,\omega'))\} \tag{2.16}$$

with Eq. (2.15) enables the wall stagnation enthalpy wave number spectrum to be determined

$$\Phi_{BB}(k,\omega)\delta(k-k')\delta(\omega-\omega')=<B(k,\omega)B^*(k',\omega')> \tag{2.17}$$

where the angle parentheses (< >) signify an ensemble average. Substituting Eqs. (2.15) and (2.16) into (2.17) gives the wall stagnation enthalpy wave number spectrum

$$\Phi_{BB}(k_{1,3},\omega)=\int_0^{+\infty} dy_2 \int_0^{+\infty} dy'_2[\int_{-\infty}^{+\infty} dk_2 e^{ik_2(y_2-y'_2)}U_1^2\frac{k_2^2}{k_1^2}(k_1^2+k_2^2+k_3^2)^2\Phi_{u_2u_2}(k_{1,2,3},\omega)]\frac{e^{iy_2\gamma(k)-iy'_2\gamma^*(k)}}{|\gamma(k)|^2} \tag{2.18}$$

where the up-wash power spectrum is also obtained as in Eq. (2.17):

$$\Phi_{u_2u_2}(k,\omega)\delta(k-k')\delta(\omega-\omega')=<\hat{u}_2(k,\omega)\hat{u}_2{}^*(k',\omega')> . \tag{2.19}$$

In order to facilitate the integration of Eq. (2.18), the up-wash wave number frequency spectrum is expressed in a separable form,

$$\Phi_{u_2u_2}(k_1,k_2,k_3,\omega)=\Phi_{u_2u_2}(\omega)\phi_1(k_1)\phi_2(k_2)\phi_3(k_3) \tag{2.20}$$

where all of the wave number spectra are normalized accordingly:

$$\int_{-\infty}^{+\infty} dk_j\phi_j(k_j)=1\ . \tag{2.21}$$

The streamwise (1) and vertical (2) wave number spectra will use Corcos'(1963) representation:

$$\phi_1(k_1)=\frac{l_1/\pi}{1+l_1^2(k_1^2-k_c^2)};\ \phi_2(k_2)=\frac{l_2/\pi}{1+l_2^2k^2};\quad l_1\approx 9U_c/\omega,\quad l_2\approx 1.4U_c/\omega\ . \tag{2.22}$$

Referring to Fig. 2.1, the convection wave number k_c= -ω/U_1 for ω>0. The sign of the convection velocity has no bearing on the value of the radiated noise power spectrum. This will become apparent since all of the subsequent expressions for the incident surface pressure spectrum involve even powers of the streamwise wave number, k_1. The spanwise (3) wave number spectrum will be approximated with a Gaussian form used by Blake (1971):

$$\phi_3(k_3)=l_3\frac{e^{-(k_3l_3/2)^2}}{2\sqrt{\pi}};\ l_3\approx 1.4U_c/\omega\ . \tag{2.23}$$

Substituting Eqs. (2.22) into Eq. (2.18) and integrating Eq. (2.18) with respect to k_2 yields:

$$\begin{aligned}\Phi_{BB}(k_{1,3},\omega)=&\int_0^{+\infty}dy_2\int_0^{+\infty}dy_2'U_1^2\Phi_{u_2u_2}(k_{1,3},\omega)]\frac{e^{iy_2\gamma(k)-iy_2'\gamma^*(k)}}{|\gamma(k)|^2}\frac{1}{k_1^2\pi}\cdot\\ &\{l_2[l_2^{-7}(e^{-(y_2-y_2')/l_2}(-1+2k_1^2l_2^2+2k_3^2l_2^2-k_1^4l_2^4-2k_1^2k_3^2l_2^4-k_3^4l_2^4)\pi)+\\ &2(-1+k_1^2l_2^2+k_3^2l_2^2)^2\pi\delta(y_2-y_2')l_2^{-6}-2(-1+k_1^2l_2^2+k_3^2l_2^2)\pi\delta''(y_2-y_2')l_2^{-4}\\ &+2\pi\delta^{iv}(y_2-y_2')l_2^{-2}]\}\end{aligned} \tag{2.24}$$

where δ^n is the nth order derivative of the delta function. The relationship between the convolution of the *n*th order derivative of the delta function, with a function, *f*, and the *n*th order derivative of *f* is given in Eq. (2.25) [Lighthill (1958)]:

$$\int_0^{+\infty} dy_2 f(y_2)\delta^n(y_2 - y_2') = (-1)^n f^n(y_2') \quad 0 < y_2' < \infty \,. \tag{2.25}$$

If the integral scale is much smaller than the spatial extent of the turbulence, then the vertical (2) correlation function can be represented as a product of the integral scale and the delta function:

$$e^{-|y_2 - y_2'|/l_2} = l_2\delta(y_2 - y_2'); l_2 \approx 1.4U_c/\omega = 1.4k_c^{-1} \,. \tag{2.26}$$

Substituting Eq. (2.26) into the expression for the wall stagnation enthalpy wave number spectrum [Eq. (2.24)] yields;

$$\begin{aligned}
&\Phi_{BB}(k_{1,3},\omega) = \int_0^{+\infty} dy_2 \int_0^{+\infty} dy_2' U_1^2 \Phi_{u_2u_2}(k_{1,3},\omega)] \frac{e^{iy_2\gamma(k) - iy_2'\gamma^*(k)}}{|\gamma(k)|^2} \frac{1}{k_1^2\pi} \cdot \\
&\{l_2[l_2^{-7}(\delta(y_2 - y_2')l_2(-1 + 2k_1^2l_2^2 + 2k_3^2l_2^2 - k_1^4l_2^4 - 2k_1^2k_3^2l_2^4 - k_3^4l_2^4)\pi) + \\
&2(-1 + k_1^2l_2^2 + k_3^2l_2^2)^2\pi\delta(y_2 - y_2')l_2^{-6} - 2(-1 + k_1^2l_2^2 + k_3^2l_2^2)\pi\delta''(y_2 - y_2')l_2^{-4} \\
&+2\pi\delta^{iv}(y_2 - y_2')l_2^{-2}]\} \,.
\end{aligned} \tag{2.27}$$

The forms of the wave number spectra in Eqs. (2.22) and (2.23) yield peak values for the streamwise and spanwise wave number spectra at $k_1 = k_c = -,+\omega/U_c$ and $k_3 = 0$, respectively. For $k_1 > k_o > k_3$, the exponential phasor in Eq. (2.27) may be approximated as:

$$\gamma(k) \approx ik_1 \,.$$

Integrating Eq. (2.27) with respect to y_2,

$$\Phi_{BB}(k_{1,3},\omega)=\int_0^{+\infty} dy_2' U_1^2 \Phi_{u_2u_2}(k_{1,3},\omega)]\frac{e^{-2k_1 y_2'}}{|\gamma(k)|^2}\frac{1}{k_1^2\pi}\cdot$$
$$\{l_2[l_2^{-7}(l_2(-1+2k_1^2l_2^2+2k_3^2l_2^2-k_1^4l_2^4-2k_1^2k_3^2l_2^4-k_3^4l_2^4)\pi)+ \qquad (2.28)$$
$$2(-1+k_1^2l_2^2+k_3^2l_2^2)^2\pi l_2^{-6}-2(-1+k_1^2l_2^2+k_3^2l_2^2)\pi 4k_1^2l_2^{-4}+2\pi 16k_1^4l_2^{-2}]\} \quad .$$

and then integrating Eq. (2.28) with respect to y_2' yields the wall stagnation enthalpy frequency wave number spectrum:

$$\Phi_{BB}(k_{1,3},\omega)=U_1^2\Phi_{u_2u_2}(k_{1,3},\omega)]\frac{1}{|\gamma(k)|^2}\frac{1}{k_1^2\pi}\cdot\frac{1}{2k_1}$$
$$\{l_2[l_2^{-7}(l_2(-1+2k_1^2l_2^2+2k_3^2l_2^2-k_1^4l_2^4-2k_1^2k_3^2l_2^4-k_3^4l_2^4)\pi)+ \qquad (2.29)$$
$$2(-1+k_1^2l_2^2+k_3^2l_2^2)^2\pi l_2^{-6}-2(-1+k_1^2l_2^2+k_3^2l_2^2)\pi 4k_1^2l_2^{-4}+2\pi 16k_1^4l_2^{-2}]\} \quad .$$

The wall stagnation enthalpy frequency spectrum is determined by integrating Eq. (2.29) with respect to k_1 and k_3. Using approximate forms of the wave number spectra of the up-wash velocity facilitates the integration. Accordingly, since the streamwise wave number spectrum of the up-wash velocity [Eq. (2.22)] is peaked at the convection ridge, and since the rest of the integrand, denoted by $f(k_1,k_3)$, of Eq. (2.29) is varying slowly in this region, the streamwise wave number spectrum shall be represented as a delta function. Thus:

$$\int_{-\infty}^{+\infty} dk_1 f(k_1,k_3)\phi_1(k_1) \approx \int_{-\infty}^{+\infty} dk_1 f(k_1,k_3)\delta(k_1-k_c)=f(k_c,k_3) \; . \qquad (2.30)$$

The wall stagnation enthalpy becomes:

$$\Phi_{BB}(k_c,k_3,\omega)=U_1^2\Phi_{u_2u_2}(\omega)\frac{l_3 e^{-(k_3l_3/2)^2}}{2\sqrt{\pi}}\frac{1}{k_c^2+k_3^2}\frac{1}{k_c^2\pi}\cdot\frac{1}{2k_c}$$
$$\{l_2[l_2^{-7}\left(l_2\left(-1+2k_c^2l_2^2+2k_3^2l_2^2-k_c^4l_2^4-2k_c^2k_3^2l_2^4-k_3^4l_2^4\right)\pi\right)+ \qquad (2.31)$$
$$2(-1+k_c^2l_2^2+k_3^2l_2^2)^2\pi l_2^{-6}-2(-1+k_c^2l_2^2+k_3^2l_2^2)\pi 4k_c^2l_2^{-4}+2\pi 16k_c^4l_2^{-2}]\} \quad .$$

Integration of the wall stagnation enthalpy wave number spectrum with respect to k_3 yields the wall point stagnation enthalpy frequency spectrum. This involves three types of integrals, $I_n(k_3)$; n=0,2,4, where

$$I_n(k_3)=\int_{-\infty}^{+\infty}\frac{k_c^2k_3^n}{k_c^2+k_3^2}\frac{l_3e^{-(k_3l_3/2)^2}}{2\sqrt{\pi}}dk_3;\ n=0,2,4\ . \tag{2.32}$$

Approximating the error function, $Erf(x)\sim x$ for $x<1$, gives the first integral, I_0 [n=0; Eq. (2.32)]

$$I_0=-e^{+(k_cl_3/2)^2}l_3\sqrt{\pi}\left(-1+Erf[1/2\sqrt{k_c^2l_3^2}]\right)k_c/2=0.6\ . \tag{2.33}$$

The second integral, I_2 [n=2; Eq. (2.32)] yields:

$$I_2=\frac{k_c}{2l_3}\{2\sqrt{k_c^2l_3^2}-e^{+(k_cl_3/2)^2}k_c^2l_3^2\sqrt{\pi}+e^{+(k_cl_3/2)^2}k_c^2l_3^2\sqrt{\pi}Erf(1/2\sqrt{k_c^2l_3^2})\}\ . \tag{2.34}$$

Numerically evaluating I_2 gives:

$$I_2=\frac{2\cdot1.12-1.36(1.12)^2\sqrt{\pi}+1.36(1.12)^2\sqrt{\pi}\cdot0.56}{2\cdot1.12\cdot k_c^{-2}}=0.4k_c^2\ . \tag{2.35}$$

The third integral, I_4 [n=4; Eq. (2.32)], becomes:

$$I_4=\frac{-l_3[-4+2k_c^2l_3^2-e^{+(k_cl_3/2)^2}\left(k_c^2l_3^2\right)^{3/2}\sqrt{\pi}+e^{+(k_cl_3/2)^2}\left(k_c^2l_3^2\right)^{3/2}\sqrt{\pi}Erf(1/2\sqrt{k_c^2l_3^2})]}{2\left(k_c^{-2}\right)^{5/2}\left(k_cl_3\right)^3}\ . \tag{2.36}$$

This simplifies to

$$I_4 = \frac{-1.12k_c^{-1}}{2k_c^{-5}(k_c l_3)^3}[-4 + 2(k_c l_3)^2 - e^{+(k_c l_3/2)^2}(k_c l_3)^3\sqrt{\pi} + e^{+(k_c l_3/2)^2}(k_c l_3)^3\sqrt{\pi}\cdot 0.56] \,. \qquad (2.37)$$

Taking

$$k_c l_3 = 1.12 \,,$$

$$I_4 = \frac{-1.12k_c^4}{2(1.12)^3}[-4 + 2(1.12)^2 - 1.36(1.12)^3\sqrt{\pi} + 1.36(1.12)^3\sqrt{\pi}\cdot 0.56] \,,$$

$$I_4 = 1.19k_c^4 \,. \qquad (2.38)$$

Substituting the three integrals, I_0, I_2, I_4 into the expression for the point stagnation enthalpy gives

$$\Phi_{BB}(\omega) = U_1^2\Phi_{u_2u_2}(\omega)\frac{1.12}{2\pi}\{(\frac{1}{(1.12)^6}[-0.6 + 2(1.12)^2 0.6 + 2(0.4)(1.12)^2 - (1.12)^4 0.6$$
$$-2(1.12)^4 0.4 - 1.19(1.12)^4]\pi)$$
$$+\frac{2\pi}{(1.12)^6}[-0.6 + 0.6(1.12)^2 + 0.4(1.12)^2]^2 \qquad (2.39)$$
$$-\frac{8\pi}{(1.12)^4}[-0.6 + 0.6\cdot(1.12)^2 + 0.4\cdot(1.12)^2] + \frac{2\pi 16\cdot 0.6}{(1.12)^2}\} \,.$$

The component of the wall stagnation enthalpy power spectrum that contributes to the lifting dipole sound expressed in terms of the mean flow velocity and the fluctuating up-wash power spectrum becomes:

$$\Phi_{BB}(\omega) = 6.4 U_1^2 \Phi_{u_2 u_2}(\omega) \, . \tag{2.40}$$

3. Dipole Sound from a Thick, Symmetric Foil in a Turbulent Flow Without Mean Shear.

In Section 2, the surface stagnation enthalpy, B, was calculated on a rigid plane due to the near field acoustic radiation from the component of Howe's (1975) acoustic source that gives rise to the lifting components of the dipoles. The source was specified to be without mean shear and was expressed in terms of the free stream velocity and the fluctuating up-wash velocity. In this section, the dipole sound, p_{rad}, due to the diffraction of these sources by the leading edge of a thick, symmetric foil will be calculated using a rigid surface Green function, $G(x,y,\omega)$ and incident "blocked" surface stagnation enthalpy, B, that satisfies the Kirchhoff equation

$$B_{rad}(x,\omega) = -\frac{1}{2}\iint_s \frac{\partial B(y_1, y_2 = 0, y_3, \omega)}{\partial y_n} G(x,y,\omega) dS(y) , \tag{3.1}$$

where B_{rad} is the far field radiated stagnation enthalpy and y_n is normal to the surface and is directed into the fluid. At low flow Mach numbers, $M_c = U/c_0 < 1$, the radiated stagnation enthalpy, B_{rad}, is related to the acoustic pressure in the far field, p_{rad}, [Howe (1978)]

$$p_{rad} = B_{rad} \cdot \rho / (1 + M_c(x_1/R)) , \tag{3.2}$$

where $M_c(x_1/R) = M_{OR}$ is the flow Mach number component in the observer direction. The acoustic pressure can then be determined in the far field from Eqs. (3.1) and (3.2):

$$p_{rad}(x,\omega) = -\frac{\rho}{2(1 + M_c(x_1/R))}\iint_s \frac{\partial B(y_1, y_2 = 0, y_3, \omega)}{\partial y_n} G(x,y,\omega) dS(y) . \tag{3.3}$$

The coordinates for the radiation field are illustrated for a foil of thickness, h, chord length, c, and span, L, in Fig. 3.1. The foil encounters homogeneous turbulence with convection velocity, $U_c = -U_1$. The cross section of the foil [Fig. 3.2(a)] shows that the turbulence flows past both sides of the leading edge of the foil. The half-plane "slab" scattering geometry that is used to model the leading edge diffraction of the incident stagnation enthalpy [Eq. (3.3)] is given in Fig. 3.2(b). The incident stagnation enthalpy is imposed by the turbulence on both sides of the

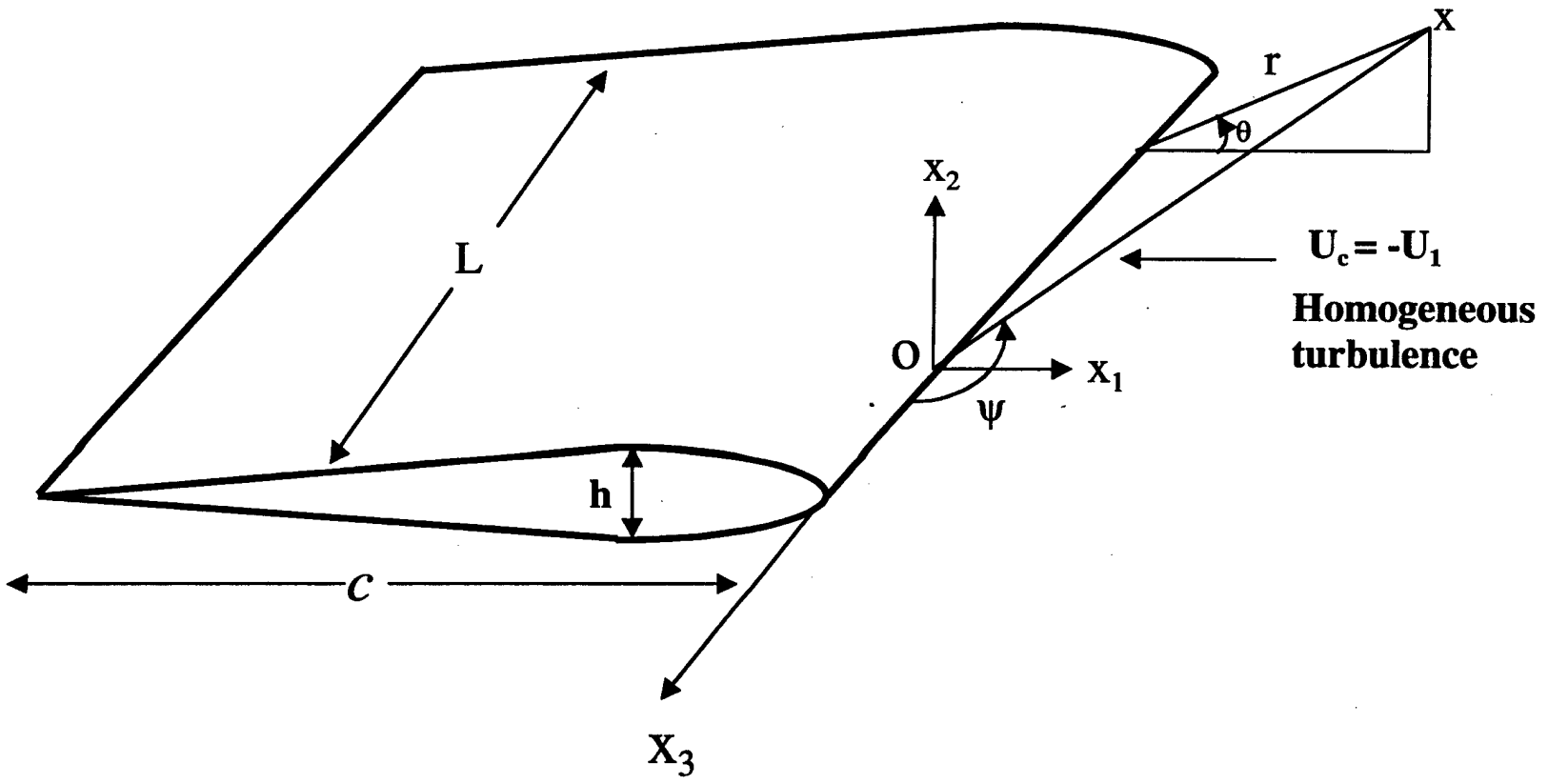

Figure 3.1 Coordinates for the acoustic field of the NACA 0012 airfoil with Span, L, thickness, h, and chord length, c, and convection velocity, U_c=-U_1

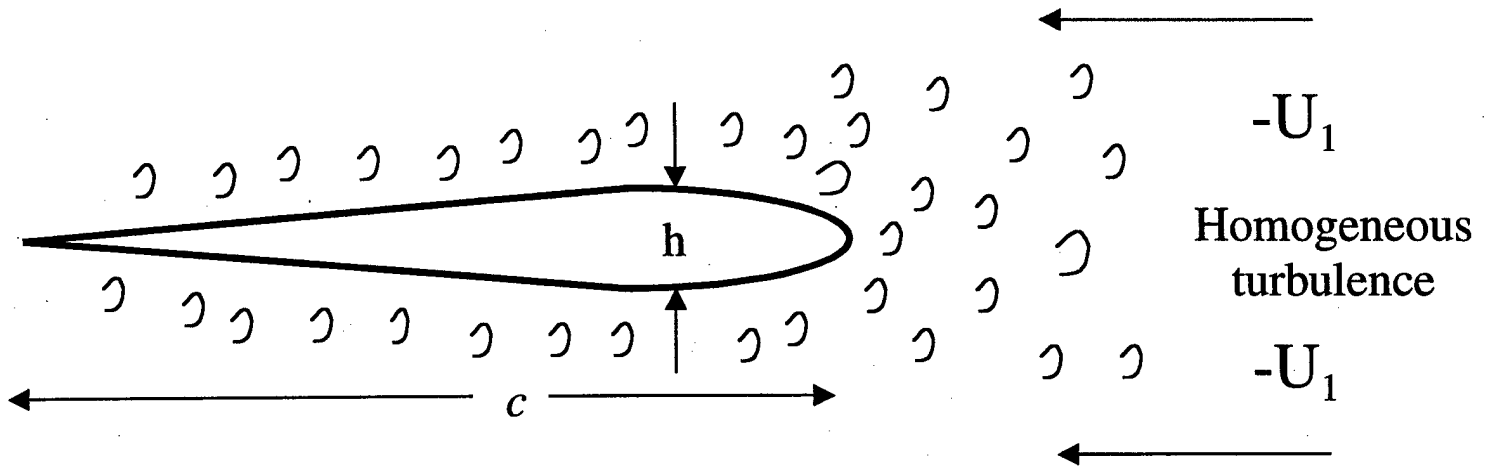

Figure 3.2 (a) NACA 0012 airfoil with chord length, c, and thickness, h, (h/c=0.12) and homogeneous, turbulent inflow with velocity, $-U_1$.

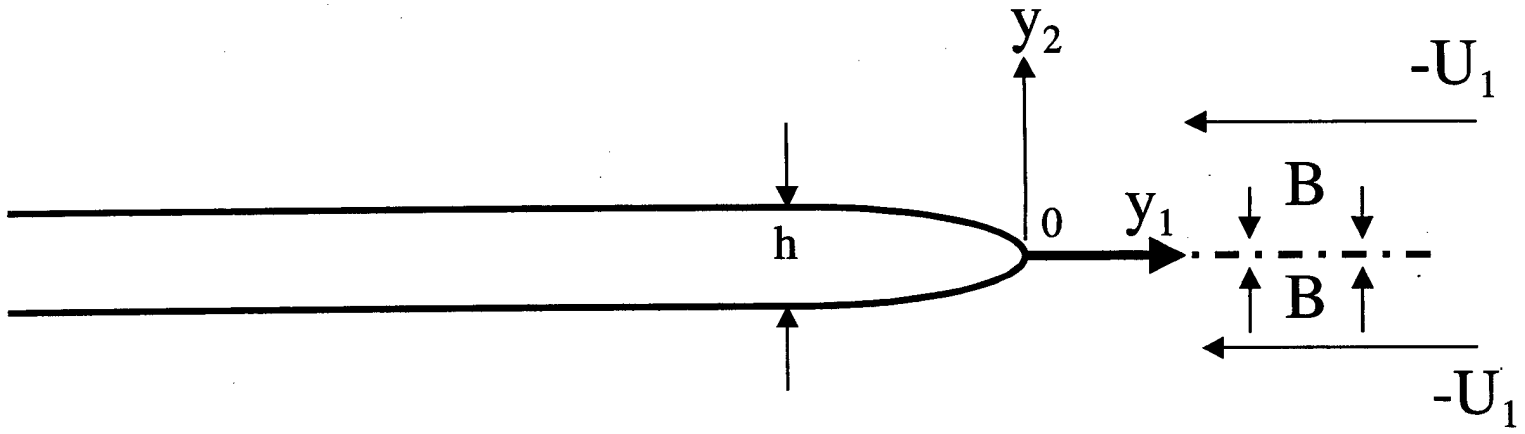

Figure 3.2 (b) Representation of the foil as a semi-infinite slab with thickness, h, and rounded leading edge for leading edge force estimate from the diffraction of the incident surface stagnation enthalpy, B.

foil. A leading edge Kutta condition is not applied and the vortical sources are prescribed to follow the potential flow streamlines associated with the foil geometry and the free stream velocity indicated in the figures. The surface of the foil is defined to have no discontinuities in the surface curvature. Even though the sources accelerate due to the curvature of the potential streamlines in the vicinity of the leading edge, it will still be assumed that the incident source wave number spectrum is peaked at the convection ridge associated with the velocity upstream of the leading edge.

The dipole sound spectrum due to the diffraction of the incident turbulence by the leading edge shall be modeled using a surface pressure scattering formulation with Howe's (1998a and b) trailing edge Green function for a semi-infinite hard surface with thickness, h and rounded edge,

$$\Phi_{PP}^{rad}(x,\omega) \approx \frac{\omega L \sin^2(\theta/2)\sin\psi}{\pi^2 c_o |x|^2} \frac{\pi}{k_c} e^{-\omega h/(2U_c)} \Phi_{PP}^{surf}(\omega) l_3(\omega)/\pi \qquad (3.4)$$

where $\Phi_{PP}^{rad}(x,\omega)$ and $\Phi_{PP}^{surf}(\omega)$ denote respectively the radiated acoustic pressure spectrum and the incident surface pressure spectrum. The right hand side of the equation has been multiplied by a factor of two in order to account for the two-sided turbulent flow around the airfoil's leading edge. Referring to Eq. (2.27), incident sources at the convection wave number, $k_c = \omega/U_c$, and location, y_2, normal to the surface have weighted contributions to the surface pressure spectrum that are exponentially attenuated by their product:

$$e^{-2\omega y_2/(U_c)}. \qquad (3.5)$$

The thickness correction, in Eq. (3.4),

$$e^{-\omega h/(2U_c)} \qquad (3.6)$$

suggests that the sound generated by a foil with thickness, h, in a spatially homogeneous turbulence field can be alternatively represented by a foil with zero thickness where the incident sources are off-set from the surface in the surface normal direction by a distance equal to one quarter of the maximum section thickness, $|y_2| > h/4$.

Substituting Eq. (2.40) that relates the mean velocity and upwash velocity to the wall pressure stagnation enthalpy and Eq. (3.5) that gives the Mach number correction into Eq. (3.6) yields the leading edge dipole sound pressure spectrum due to the diffraction of the homogeneous turbulence:

$$\Phi_{PP}^{rad}(x,\omega) \approx \frac{\omega L \sin^2(\theta/2)\sin\psi}{(1+M_{OR})^2 \pi^2 c_o |x|^2} \frac{\pi}{k_c} e^{-\omega h/(2U_c)} 6.4\rho^2 U_1^2 \Phi_{u_2u_2}(\omega) l_3(\omega)/\pi \,. \qquad (3.7)$$

The multiple "back-scattering" of the acoustic waves generated by the leading edge diffraction of the turbulence by the edges of the foil occur when the chord length is finite but acoustically non-compact. Howe's (2001a) normalized Green function, G_T, shall be used to model this effect. This yields an equation for the dipole sound from the thick but acoustically non-compact airfoil in terms of the mean velocity and the up-wash velocity spectrum and spanwise integral scale:

$$\Phi_{PP}^{rad}(x,\omega) \approx \frac{|G_T(k_o c \sin(\psi))|^2}{(1+M_{OR})^2} \frac{\omega L \sin^2(\theta/2)\sin\psi}{\pi^2 c_o |x|^2} \frac{\pi}{k_c} e^{-\omega h/(2U_c)} 6.4\rho^2 U_1^2 \Phi_{u_2u_2}(\omega) l_3(\omega)/(\pi) \,. \qquad (3.8)$$

The normalized Green function is given by

$$G_T(x,y,\omega) = 1 + \frac{G_{LE}(x,y,\omega) + G_{TE}(x,y,\omega)}{G_{1/2\,plane}(x,y,\omega)} \,, \qquad (3.9)$$

where G_{LE}, G_{TE}, $G_{1/2plane}$ represent respectively, the contributions from the leading edge, the trailing edge and the governing Green function for the "half- slab" diffracting surface used in Eq. (3.7). These are given by Howe (2001) with [Fig. (3.1)] $\theta=\psi=\pi/2$:

$$G_{TE}(x,y,\omega) \approx \frac{-\varphi^*(y) e^{ik_o(|x'|)}}{\pi^2 \sqrt{2ic}\,|x|[1+e^{2ik_o c}/(2\pi i k_o c)]} F\left(2\sqrt{k_o c \cos^2(\pi/4)/\pi}\right) , \qquad (3.10)$$

$$G_{LE}(x,y,\omega) \approx \frac{\sqrt{k_o}\sin^{1/2}(\psi)\varphi^*(y)e^{ik_o(|x'|)}}{i\pi^{3/2}|x|[1+e^{2ik_oc}/(2\pi ik_oc)]}F\left(2\sqrt{k_oc\cos^2(\pi/4)/\pi}\right). \tag{3.11}$$

$F(x) = f(x) + ig(x)$ are the Fresnel integral auxiliary functions whose approximations are given by:

$$f(x) = \frac{1+0.926x}{2+1.792x+3.104x^2}; g(x) = \frac{1}{2+4.142x+3.492x^2+6.67x^3}. \tag{3.12}$$

The predicted dipole sound from Eq. (3.8) shall be compared with the measured sound reported by Paterson and Amiet (1976) in Fig. 1.1. Accordingly, the reported up-wash spectrum will use the von Karman formulation for isotropic turbulence with an integral scale, λ_f= 0.03 m, and a turbulence intensity, $u^2/U^2 = 0.045$,

$$\Phi_{u_2u_2}(\omega) = \frac{\overline{u^2}\lambda_f}{2\pi U}\frac{[1+\frac{8}{3}(k_c4\lambda_f/3)^2]}{[1+(k_c4\lambda_f/3)^2]^{\frac{11}{6}}}. \tag{3.13}$$

The spanwise integral scale, $l_3(\omega)$ will also use the von Karman formulation,

$$l_3(\omega) = \frac{8}{3}\left[\frac{\Gamma(1/3)}{\Gamma(5/6)}\right]^2\lambda_f\frac{(4\lambda_fk_c/3)^2}{[3+8(4\lambda_fk_c/3)^2]\sqrt{1+(4\lambda_fk_c/3)^2}}, \tag{3.14}$$

yielding the same result as the Corcos model or the Gaussian model for frequencies above 300 Hz. Γ is the Gamma function with $\Gamma(1/3)$=2.68, and $\Gamma(5/6)$=1.13.

The airfoil chord length is c= 0.23 m, the span is L=0.53 m. The thickness (h) to chord (c) ratio of the NACA foil is h/c=0.12. The dipole sound in Fig. 1.1 was measured at a distance x_2=2.25 m from the mid-chord of the foil. The Mach number correction in Eq. (3.2) becomes, M_{OR}=0.05 M_c and $\theta=\psi=\pi/2$. In Fig. 3.3 for h/c =0 and in Fig. 3.4 for h/c =0.12, the predicted dipole sound spectra are plotted using Eq. (3.8) at velocities of 40m/s, 60 m/s, 90 m/s and 120 m/s. These predictions are compared at each velocity to the measured dipole sound from Paterson and Amiet (1976, 1977).

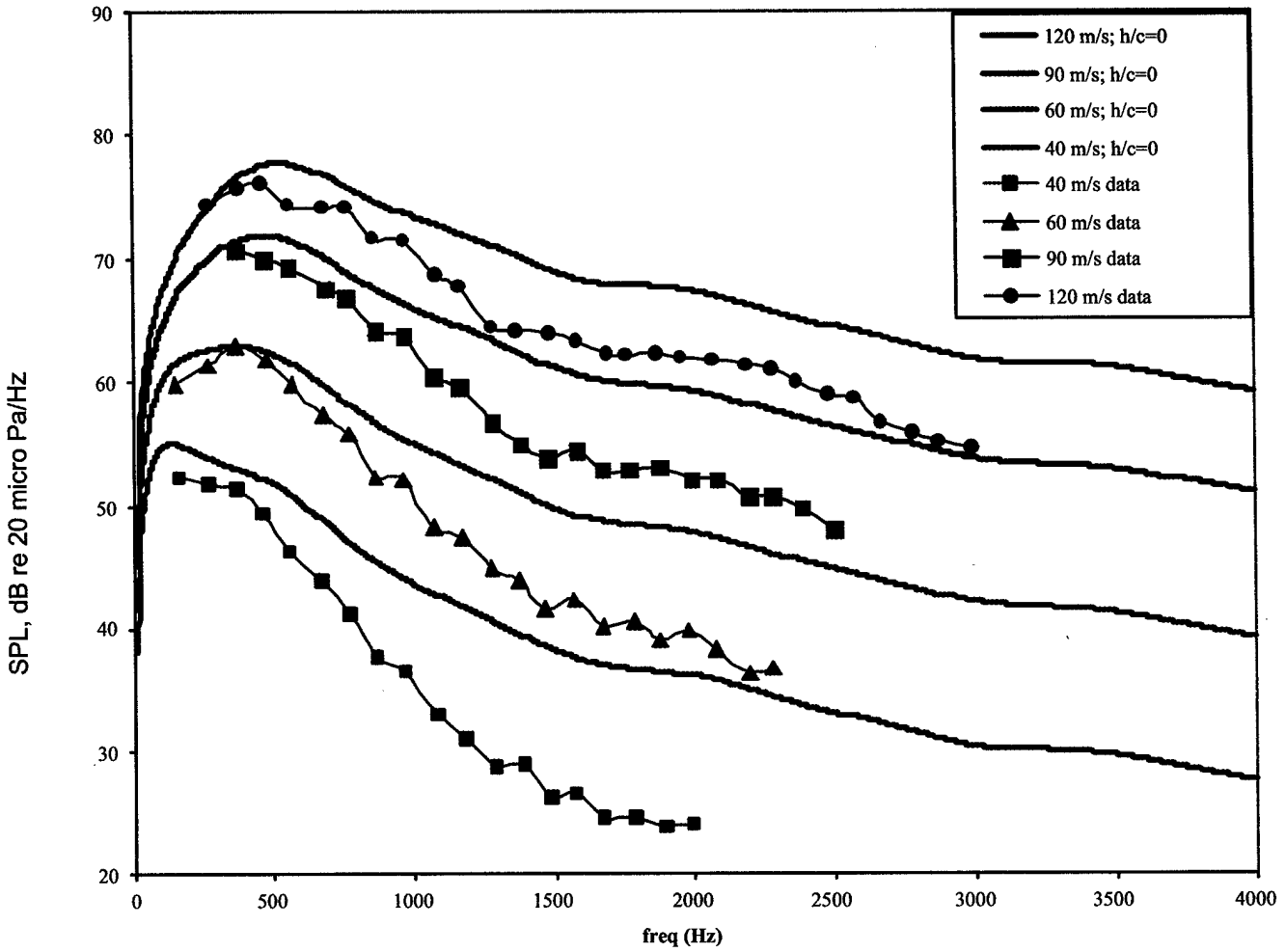

Figure 3.3 A comparison of the NACA 0012 (h/c=0.12) dipole sound measurements of Paterson and Amiet (1976, 1977) (points), and the thickness theory [Eq. (3.8)] with h/c=0.0 (line) for free stream velocities of 40 m/s, 60 m/s, 90 m/s, and 120 m/s.

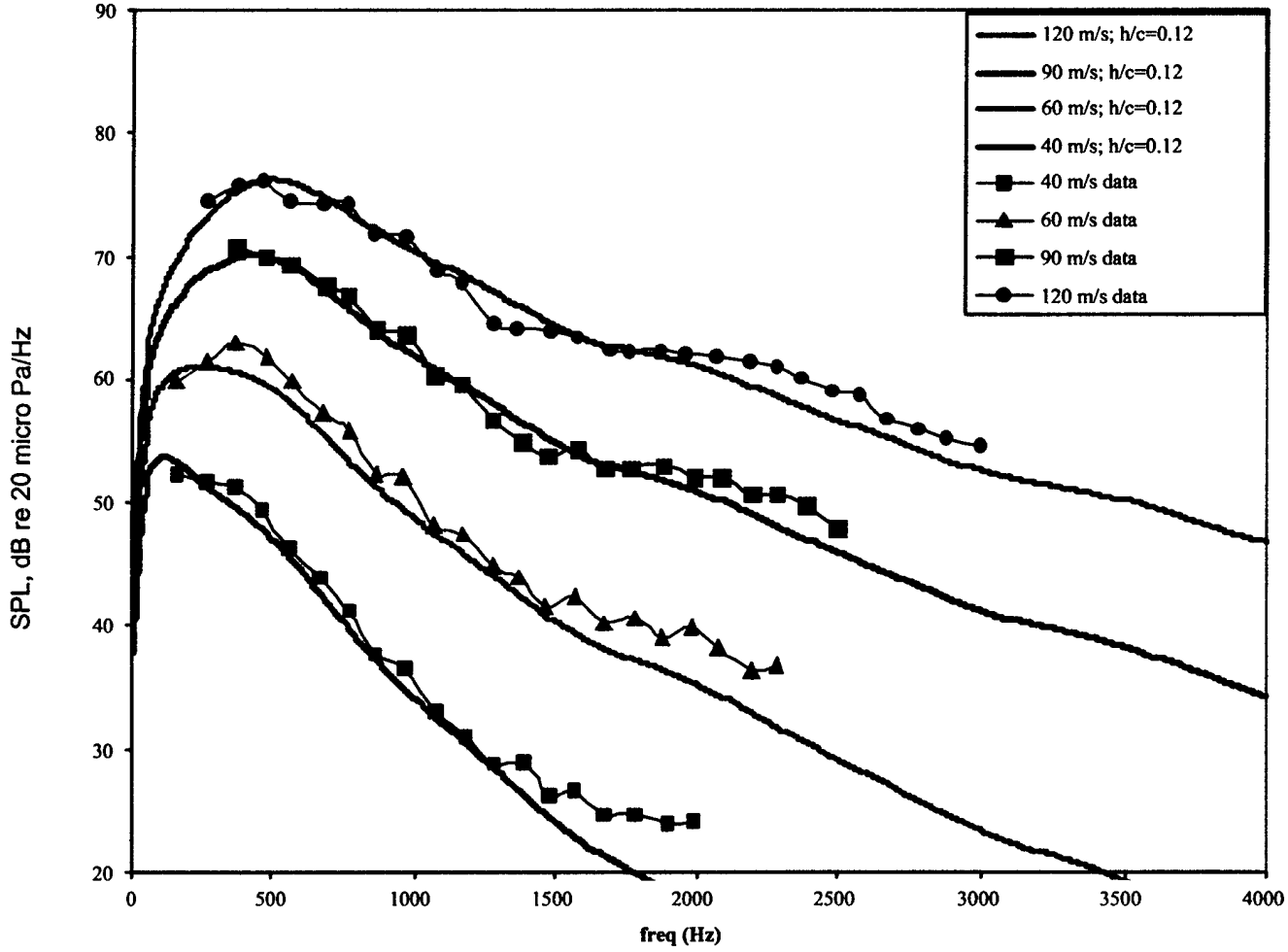

Figure 3.4 A comparison of the NACA 0012 (h/c=0.12) dipole sound measurements of Paterson and Amiet (1976, 1977) (points), and the thickness theory [Eq. (3.8)] with h/c=0.12 (line) for free stream velocities of 40 m/s, 60 m/s, 90 m/s, and 120 m/s.

4. Dipole Sound From a Thick, Symmetric Foil in a Turbulent Flow With Mean Shear.

In Section 1, the turbulence quadrupole source was specified to be without mean shear. These types of turbulent flows are typically generated by turbulent wake flows and jet induced shear layers that have had sufficient time to diffuse or by the outer portion of a turbulent boundary layer (TBL) flow. Conversely, wake and jet flows have regions of high mean shear before sufficient diffusion occurs, as do turbulent flows near their bounding surfaces. The portion of the acoustic source that contains the mean shear–turbulent (MS-T) source has been used to describe the quadrupole pressure radiation from turbulent shear flows that occur in TBL flows [Kraichnan (1956), Chase (1980), Blake (1986)] and jets [Moon (1975)]. In this section, the dipole sound due to a MS-T source incident to the leading edge of a thick foil will be modeled.

Referring to Fig. 4.1(a), a foil of thickness, h, and chord length, c, encounters a turbulent shear layer, $dU_1(y_2)/dy_2$=const., where the shear layer is thicker than the foil thickness. The force induced by the diffraction of the turbulent shear layer by the leading edge is formulated as a Kirchhoff integral for the scattering of the incident surface pressure by a "semi-infinite slab" with thickness, h, and rounded leading edge [Fig. 4.1(b)]. The modeling approach is identical to that described in Sections 2 and 3. In this section, the wall pressure spectrum imposed on a rigid plane will be calculated from the quadrupole radiation of the aero-acoustic source that has been specialized to be linear in fluctuating terms and to contain mean shear. This pressure spectrum can be used with the results of Section 2 to calculate the leading edge noise for a thick foil cutting through a shear layer that will be specialized to be spatially homogeneous.

At low Mach numbers, the acoustic pressure, $\mathbf{p}$, generated by the mean shear-turbulence (MS-T) source is described by the following acoustic analogy:

$$\frac{1}{c_o^2}\frac{\partial^2 \mathbf{p}}{\partial t^2} - \nabla^2 \mathbf{p} \approx 2\rho_o \frac{\partial U_1}{\partial y_2}\frac{\partial \mathbf{u}_2'}{\partial y_1} . \tag{4.1}$$

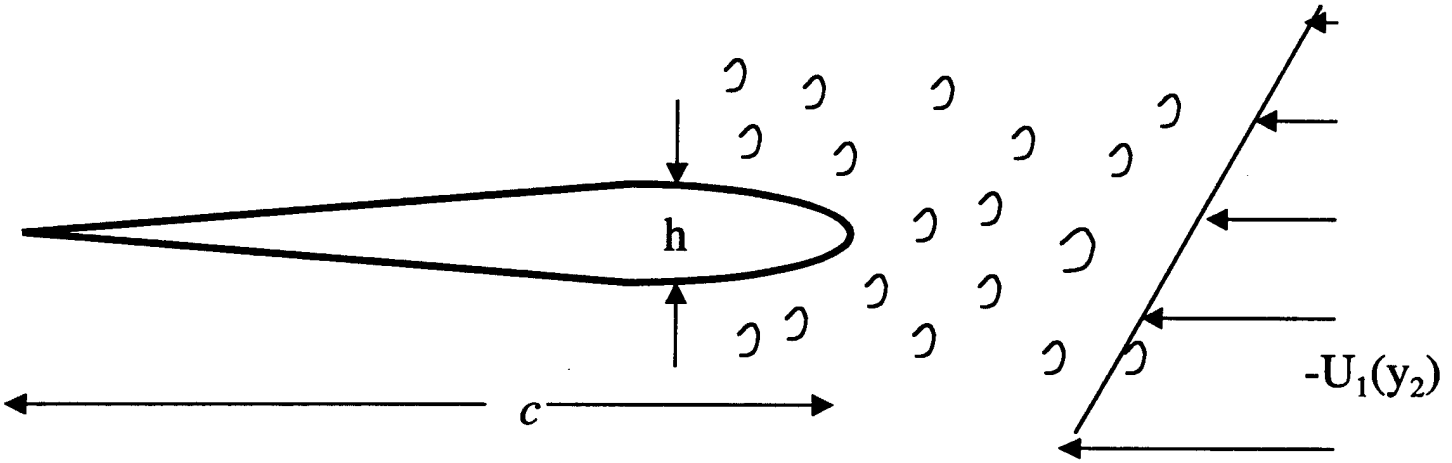

Figure 4.1 (a) Foil with chord length, c, and thickness, h, and homogeneous turbulent inflow with mean shear, dU_1/dy_2=const.

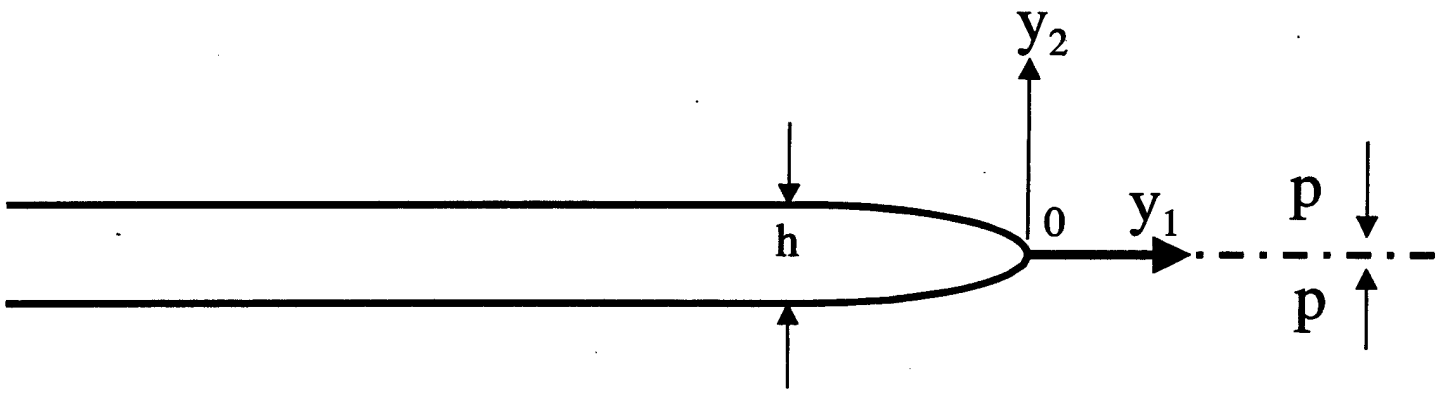

Figure 4.1 (b) Representation of foil as a semi-infinite slab, with thickness, h, and rounded leading edge for leading edge force estimate due to diffraction of incident surface pressure, p.

The pressure, p, and the fluctuating up-wash velocity, $\dot{u_2}$, are in the time domain and are denoted by bold face type. The planar wave number spectrum of the wall pressure that is radiated by the acoustic source in Eq. (4.1) becomes

$$p(k,\omega)=\frac{1}{(2\pi)^2}\iiint_V dV(y)2\rho_o\frac{\partial U_1(y)}{\partial y_2}\frac{\partial \dot{u}_2(y,\omega)}{\partial y_1}\iint_S dx\frac{e^{-ik\cdot x+ik_o r}}{r} \tag{4.2}$$

where the pressure, p, and up-wash velocity, u_2, have been Fourier transformed to the frequency domain and are no longer in bold face type.

The planar Fourier transform of the Green Function is given by

$$\frac{1}{2\pi}\iint_{-\infty}^{+\infty}\frac{e^{ik_0 r}}{r}e^{-ik_{1,3}\cdot x_{1,3}}d^2x_{1,3}=i\frac{e^{iy_2\gamma(k)}}{\gamma(k)}e^{-ik_{1,3}\cdot y_{1,3}} \tag{4.3}$$

where

$$\gamma(k)=\sqrt{k_o^2-k_1^2-k_3^2} \tag{4.4}$$

and $k_o = \omega/c_o$, $k_{1,3}=(k_1,k_3)$, $y_{1,3}= (y_1,y_3)$, $x_{1,3}= (x_1,x_3)$, $d^2x_{1,3}=dx_1dx_3$. Substituting Eq. (4.3) into the Eq. (4.2),

$$p(k,\omega)=\frac{1}{(2\pi)^2}\iiint_V dy_2dy_{1,3}e^{-ik_{1,3}\cdot y_{1,3}}2\rho\frac{\partial U_1}{\partial y_2}\frac{\partial \dot{u}_2}{\partial y_1}(y_1,y_2,y_3,\omega)i\frac{e^{iy_2\gamma(k)}}{\gamma(k)} \tag{4.5}$$

and rearranging the terms of the integrand gives the following expression for the wall pressure wave number spectrum:

$$p(k,\omega)=\frac{1}{(2\pi)^2}\int_{y_2=0}^{\infty}dy_2 2\rho\frac{\partial U_1}{\partial y_2}i\frac{e^{iy_2\gamma(k)}}{\gamma(k)}\iint_{y_1y_3=-\infty}^{+\infty}d^2y_{1,3}e^{-ik_{1,3}\cdot y_{1,3}}\frac{\partial \dot{u}_2}{\partial y_1}(y_1,y_2,y_3,\omega)\ . \tag{4.6}$$

The Fourier transform of the fluctuating up-wash velocity with respect to the in-plane coordinates is denoted by an over bar

$$\overline{u_2'}(k_{1,3},y_2,\omega)=\iint_{-\infty}^{+\infty} d^2y_{1,3}\frac{1}{(2\pi)^2}e^{-ik_{1,3}\cdot y_{1,3}}u_2'(y_1,y_2,y_3,\omega) \tag{4.7}$$

and Fourier transform of the derivative of the up-wash velocity is:

$$ik_1\overline{u_2'}(k_{1,3},y_2,\omega)=\iint_{-\infty}^{+\infty} d^2y_{1,3}\frac{1}{(2\pi)^2}e^{-ik_{1,3}\cdot y_{1,3}}\frac{\partial u_2'(y_1,y_2,y_3,\omega)}{\partial y_1}\,. \tag{4.8}$$

Substituting Eq. (4.8) into Eq. (4.6) determines the wall pressure wavenumber spectrum

$$p(k,\omega)=\int_{y_2=0}^{\infty} dy_2 2\rho\frac{\partial U_1}{\partial y_2}i\frac{e^{iy_2\gamma(k)}}{\gamma(k)}ik_1\overline{u_2'}(k_1,y_2,k_3,\omega) \tag{4.9}$$

and the complex conjugate of the wall pressure spectrum becomes:

$$p^*(k',\omega')=\int_{y_2=0}^{\infty} dy'_2 2\rho\frac{\partial U'_1}{\partial y'_2}(-i)\frac{e^{-iy'_2\gamma^*(k)}}{\gamma^*(k)}(-ik_1)\overline{u_2'}(k'_1,y'_2,k'_3,\omega')\,. \tag{4.10}$$

The wall pressure power spectrum is then determined from the ensemble average of the pressure and its complex conjugate:

$$\Phi_{pp}(k,\omega)\delta(k-k')\delta(\omega-\omega')=<p(k,\omega)p^*(k',\omega')> \tag{4.11}$$

yielding the wall pressure wave number frequency spectrum :

$$\Phi_{pp}(k_{1,3},\omega)=4\rho^2\int_0^{+\infty}dy_2\int_0^{+\infty}dy'_2\frac{\partial U_1'(y'_2)}{\partial y'_2}\frac{\partial U_1(y_2)}{\partial y_2}k_1^2\Phi_{u_2u_2}(k_{1,3},y_2,y'_2,\omega)]\frac{e^{iy_2\gamma(k)-iy'_2\gamma^*(k)}}{|\gamma(k)|^2}\,. \tag{4.12}$$

The following separable form to the up-wash wave number spectrum,

$$\Phi_{u_2u_2}(k_1, y_2, y_2', k_3, \omega) = \Phi(\omega)\phi_1(k_1)R_{22}(y_2, y_2')\phi_3(k_3) \tag{4.13}$$

will facilitate the integration of Eq. (4.12). The wave number spectra are normalized

$$\int_{-\infty}^{+\infty} dk_j \phi_j(k_j) = 1 \tag{4.14}$$

and the streamwise (1) and spanwise (3) wave number spectra will use Corcos' (1963) and a Gaussian form respectively:

$$\phi_1(k_1) = \frac{l_1/\pi}{1 + l_1^2(k_1^2 - k_c^2)};\ \phi_3(k_3) = l_3 \frac{e^{-(k_3 l_3/2)^2}}{2\sqrt{\pi}};\ l_3 \approx 1.4U_c/\omega\,. \tag{4.15}$$

The shear layer will be considered to be much thicker than the airfoil. In this context, this model will assume that the surface normal correlation length, l_2=$1.4U_c/\omega$, is much smaller than the thickness of the shear layer. The surface normal correlation function will accordingly be taken to be spatially homogeneous with correlation length l_2:

$$R_{22}(y_2, y_2', \omega) = \delta(y_2 - y_2')l_2(\omega)\,. \tag{4.16}$$

It is specified that the mean shear does not change significantly over the correlation length, l_2. Upon insertion of Eqs. (4.13), (4.15) and (4.16) into Eq. (4.12) and integrating with respect to y_2', the wall pressure wavenumber spectrum becomes:

$$\Phi_{pp}(k_{1,3}, \omega) = 4\rho^2 \int_0^{+\infty} dy_2 k_1^2 \left(\frac{\partial U_1(y_2)}{\partial y_2}\right)^2 \Phi_{u_2u_2}(\omega)\phi_1(k_1)\phi_3(k_3)l_2(\omega)\frac{e^{iy_2\gamma(k) - iy_2\gamma^*(k)}}{|\gamma(k)|^2}\,. \tag{4.17}$$

The wall pressure frequency spectrum is determined by integrating over k_1 and k_3. Integration over the streamwise wave number, k_1, is facilitated by assuming that the correlation function in the streamwise direction is peaked at the convection ridge, $k_1 = k_c$. The streamwise wavenumber spectrum can be approximated by a delta function

$$\phi_1(k_1) \approx \delta(k_1 - k_c) \,, \tag{4.18}$$

yielding

$$\int dk_1 \Phi_{pp}(k_{1,3},\omega) = 4\rho^2 \int_0^{+\infty} dy_2 k_c^2 \left(\frac{\partial U_1(y_2)}{\partial y_2} \right)^2 \Phi_{u_2 u_2}(\omega) \phi_3(k_3) l_2(\omega) \frac{e^{iy_2\gamma(k_c) - iy_2\gamma^*(k_c)}}{|\gamma(k_c)|^2} \,, \tag{4.19}$$

where

$$\gamma(k_c) = \sqrt{k_0^2 - k_c^2 - k_3^2} \approx i\sqrt{k_c^2 + k_3^2} \,. \tag{4.20}$$

Substitution of Eq. (4.20) into (4.19) gives the spanwise wall pressure wave number spectrum

$$\Phi_{pp}(k_3,\omega) = 4\rho^2 \int_0^{+\infty} dy_2 k_c^2 \left(\frac{\partial U_1(y_2)}{\partial y_2} \right)^2 \Phi_{u_2 u_2}(\omega) \phi_3(k_3) l_2(\omega) \frac{e^{-y_2[2\sqrt{k_c^2 + k_3^2}]}}{k_c^2 + k_3^2} \,. \tag{4.21}$$

The spanwise wave number spectrum is peaked at k_3=0. This allows the spanwise wave number correlation coefficient to be approximated by a delta function:

$$\phi_3(k_3) \approx \delta(k_3) \,. \tag{4.22}$$

Insertion of Eq. (4.22) into (4.21) yields Eq. (4.23):

$$\int dk_3 \Phi_{pp}(k_3,\omega) = 4\rho^2 \int_0^{+\infty} dy_2 \left(\frac{\partial U_1(y_2)}{\partial y_2} \right)^2 \Phi_{u_2 u_2}(\omega) e^{-y_2 2k_c} l_2(\omega) \int_{-\infty}^{+\infty} dk_3 \frac{\delta(k_3) k_c^2}{k_c^2 + k_3^2} \,. \tag{4.23}$$

Integration over the spanwise wave number yields the wall pressure frequency spectrum,

$$\Phi_{pp}(\omega) = 2\rho^2 \int_0^{+\infty} dy_2 \left(\frac{\partial U_1(y_2)}{\partial y_2} \right)^2 \Phi_{u_2 u_2}(\omega) e^{-y_2 2k_c} l_2(\omega) \tag{4.24}$$

and integrating with respect to y_2 yields the point pressure spectrum for the mean shear source:

$$\Phi_{pp}(\omega) = \rho^2 \left(\frac{\partial U_1(y_2)}{\partial y_2} \right)^2 \Phi_{u_2 u_2}(\omega) k_c^{-1} l_2(\omega) \ . \tag{4.25}$$

The ratio of the point pressure spectrum from the mean shear-turbulence (MS-T) source [Eq. (4.25)] to the source without mean shear (T-T) [Eq. (2.39)] is:

$$\frac{\Phi_{pp}^{MS-T}(\omega)}{\Phi_{pp}^{T-T}(\omega)} \approx \left(\frac{\partial U_1}{\partial y_2} \frac{1}{4.6\omega} \right)^2 . \tag{4.26}$$

This defines a cut-off frequency below which the dipole sound from the MS-T source should dominate the dipole sound from the source without mean shear (T-T).

The leading edge dipole sound is determined by multiplying the ratio of the MS-T wall pressure spectrum to the T-T spectrum [Eq. (4.26)] by the dipole sound due to the T-T source [Eq. (3.8)]:

$$\begin{aligned} \Phi_{PP}^{rad\ MS-T}(x,\omega) \approx & \frac{|G_T(k_o c \sin(\psi))|^2}{(1+M_{OR})^2} \frac{\omega L \sin^2(\theta/2) \sin\psi}{\pi^2 c_o |x|^2} \frac{\pi}{k_c} e^{-\omega h/(2U_c)} \cdot \\ & \cdot \left(\frac{\partial U_1}{\partial y_2} \frac{1}{4.6\omega} \right)^2 6.4\rho^2 U_1^2 \Phi_{u_2 u_2}(\omega) l_3(\omega)/(\pi) \ . \end{aligned} \tag{4.27}$$

The dipole sound measurements made by Olsen and Wagner (1982) with airfoils in the shear layer of a 10 cm diameter round jet will be predicted using estimates of the incident

sources with and without mean shear from equations [Eq. (4.27)] and [Eq. (3.8)] respectively. The chord length, c, of the foil was 2.54 cm. It will be assumed that the wetted span of the airfoil, L, was equal to the jet diameter. The airfoil thickness to chord ratio ranged from $0.032 < h/c < 0.375$. The flow speed incident to the leading edge of the foil was 94 m/s and the integral scale was l_f=1.6 cm. The fluctuating velocity was 25% of the mean velocity incident to the leading edge of the foil. The mean shear, dU_1/dy_2=1723/sec was estimated from the mean velocity measurements of Wygnanski and Fiedler (1965) for a round self-similar jet. The sound pressure levels in one-third octave frequency bandwidths were measured at roughly $y_2 = 4.57$ m with $\theta = \psi = \pi/2$ from Fig. 3.1. The leading edge of the foil was four jet diameters downstream of the lip of the jet.

The predicted narrow band sound pressure levels in dB re 20 micro Pa/Hz for both sources are plotted in Fig. 4.2 for a flow speed of 94 m/s. The predicted dipole sound spectrum from the mean shear source dominates below 100Hz. The dipole sound without the mean shear source is predicted for foil thickness-to-chord ratios of h/c= 0.032 and 0.375. Above 1 kHz, the thickness effect starts to attenuate the predicted dipole sound.

Figure 4.3 shows the measured dipole sound from Olsen and Wagner (1982, Fig. 2a) in one -third octave bandwidths. The thickness theory accounts for the relative differences in the dipole sound for the foils as a function of thickness. The dipole sound is not measured below 200 Hz where the predicted mean shear dipole sound should dominate. This may explain why the theory used by Olsen and Wagner (1982) was able to predict the leading edge noise for the thin airfoil without taking into account the mean shear source. The predictions made in Fig. 4.2 violate the "rapid distortion" approximation since the turbulence levels are above 10%. The mean shear levels were estimated assuming self-similarity of the mean velocity profiles even for distances downstream of the jet exit as close as four jet diameters.

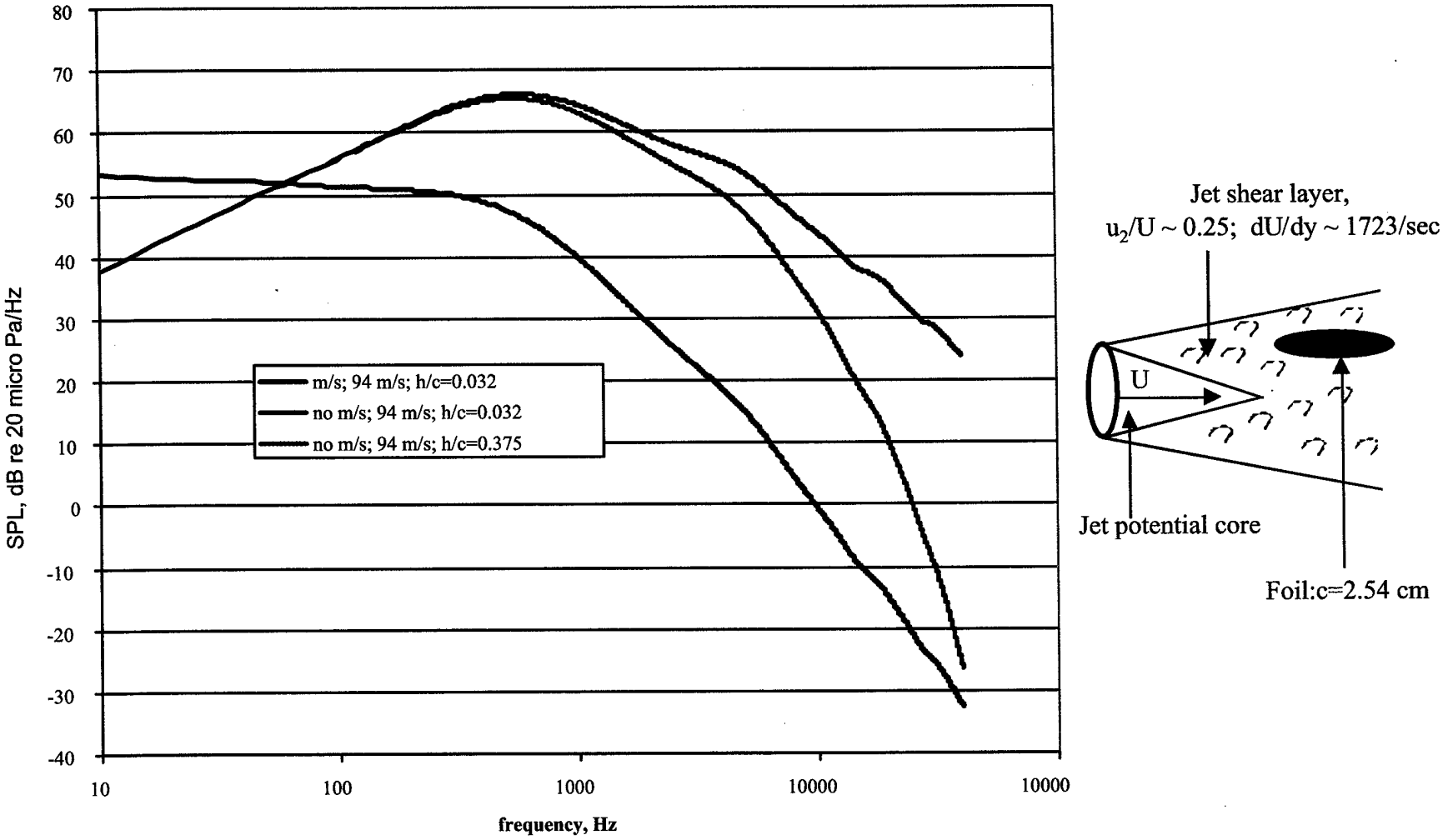

Figure 4.2 Predicted leading edge dipole sound pressure, dB re 20 micro Pa/Hz at 94 m/s with mean shear source (m/s) for h/c=0.032 (blue) and without mean shear (no m/s) for h/c-0.032 (red), 0.375 (green).

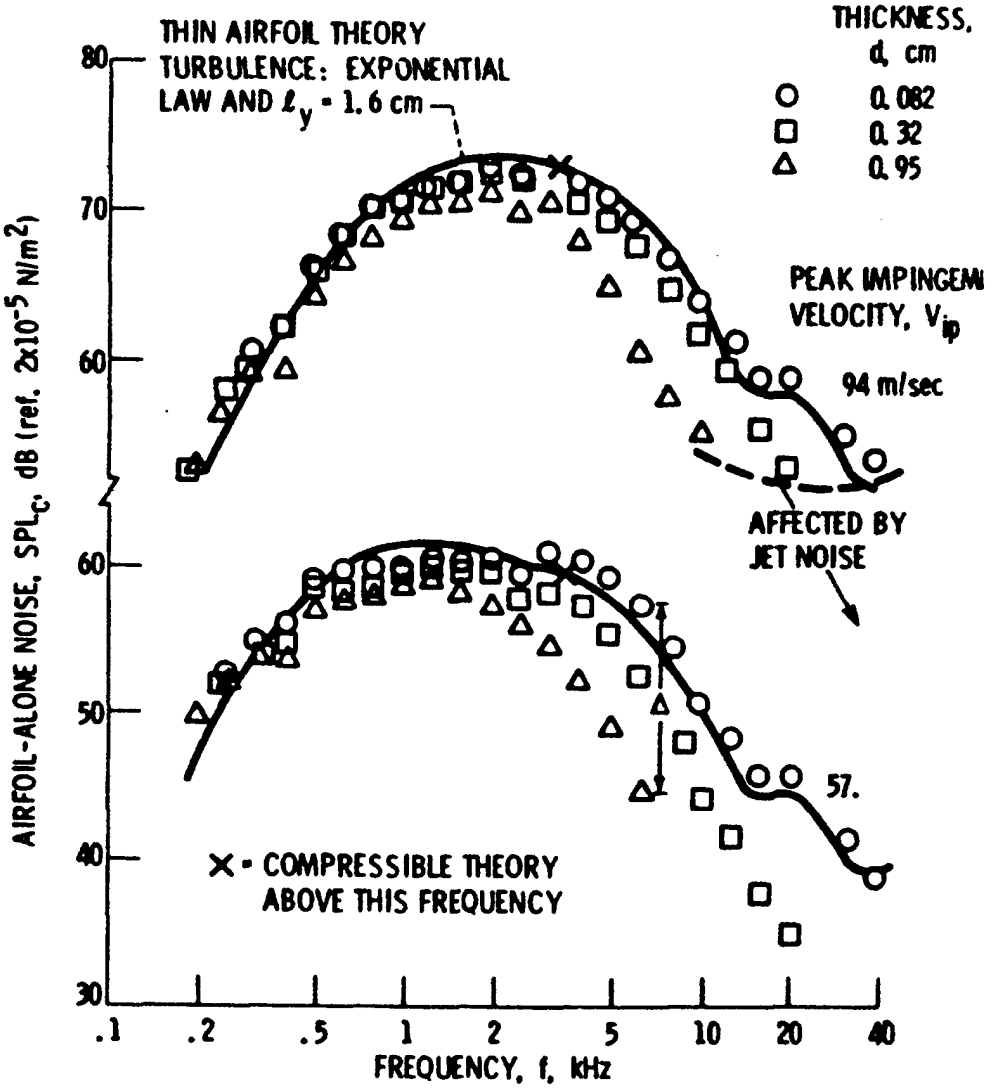

Figure 4.3 Measured dipole sound at 94 m/s in one-third octave bands, dB re 20 micro Pa (Fig. 2a, Olsen and Wagner, AIAA 82-4068).

5. Conclusions

The dipole sound due to the diffraction of homogeneous turbulence by the leading edge of a thick foil was calculated using the Kirchhoff surface integral with a rigid surface Green function. The Green function accounted for the foil thickness and the acoustic back scattering associated with the acoustically non-compact chord length. The surface stagnation enthalpy was calculated with a volume integral incorporating the rigid plane Green function and an equivalent form of the lifting dipole component of Howe's (1975) acoustic source that was derived in terms of the mean free stream velocity and the fluctuating up-wash velocity of Sears' (1941) analysis. The derivation of the equivalent form of the source required that the velocity field be solenoidal.

An estimate of the dipole radiation was made using the foil geometry and measured grid-generated turbulence statistics from Paterson and Amiet (1976, 1977). The predictions show good agreement with the measured dipole sound. This establishes that the square of the magnitude of Sears' function, $S(k_1,h)$, for a foil of thickness, h, can be expressed as

$$|S(k_1,h)|^2 = |S(k_1)|^2 \exp[-k_1 h/2], \tag{5.1}$$

where $S(k_1)$ is Sears' function with h=0.

The modeling approach requires that the incident sources obey the "rapid distortion" approximation. This requirement may be violated when the turbulence fluctuations are too large relative to the free stream geometry. When this occurs, the sources may interact with each other or their images. The RMS turbulence fluctuations of the validation data of Paterson and Amiet (1976, 1977) were approximately 4.5% of the free stream. This is well within the limits (less than 10%) established by Grace (2001) to ensure that the sources do not deviate from the potential flow. Leading edge flow separation from a sharp edge may also cause the trajectories of the incident sources to deviate sufficiently from that modeled by the Green function. This modeling approach also required the use of the frozen flow approximation that is strictly applicable to constant velocity flows in the vicinity of the diffraction zones. The success of the dipole sound predictions suggests that the frozen flow approximation may be applied to steady flows whose potential flow streamlines exhibit curvature and consequential acceleration of the sources around an edge. Extensions of the modeling approach can be made to predict the affect

of foil camber on the dipole sound by incorporating this effect into the velocity potential of the Green function via a conformal mapping, as demonstrated by Martinez and Rudzynsky (1997) for the incompressible problem.

The dipole sound from a foil cutting through a mean shear layer was obtained using the acoustic source that was tailored for mean shear sources. The incident surface pressure spectrum due to this source that is imposed on a rigid plane was calculated. The ratio of the dipole sound of the mean shear source to the source without mean shear was determined to be proportional to the square of the ratio of the mean shear to the frequency of the sources. This establishes a critical frequency below which the dipole sound from the mean shear should dominate and above which the dipole sound from the source without mean shear should dominate. This result has been reported for the frequency dependence of the mean shear and non-mean shear quadrupole sources associated with jet radiation (e.g., Moon (1975)).

Estimates of the measured leading edge dipole sound by Olsen and Wagner (1982) were made with and without the mean shear incident sources. The frequency below which the mean shear source was estimated to dominate was 100Hz. The measured dipole sound was made for frequencies above 200 Hz. This may explain why the predicted dipole sound made by Olsen and Wagner (1982) agreed with the measurements even though they did not take into account the mean shear source.

References

Adamczyk, J.J., "The passage of an infinite swept airfoil through an oblique gust," NASA CR-2395 (1974).

Amiet, R.K., "Acoustic Radiation from an Airfoil in a Turbulent Stream," J. Sound and Vib, 41(4), 407-420 (1975).

Blake, W.K., Mechanics of flow-Induced Sound and Vibration V.1&V.2, Academic Press (1986).

Blake,W.K., "Turbulent Velocity and Presure Fields in Boundary-Layer Flows over Rough Surfaces," Proceedings of the Symposium on Turbulence in Liquids, Univ. Missouri-Rolla (Oct. 1971).

Chase, D.M., "Modeling of Wavevector-Frequency Spectrum of Turbulent Boundary Layer Wall Pressure," J. Sound and Vibration, Vol. 70, No. 1, pp. 29-67,(1980).

Corcos,G.M.," The resolution of pressure in turbulence," J. Acoust. Soc. Am. 35, pp. 192-199 (1963).

Grace, S.M. "Unsteady blade response: the BVI model vs. the gust model,' AIAA 2001-2209, 7th AIAA/CEAS Aeroacoustics Conference, May 28-30, 2001/ Maastricht, The Netherlands (2001).

Howe, M.S. "Contributions to the theory of aerodynamic sound, with application to excess jet noise and the theory of the flute," J. Fluid Mech..71(4),pp. 625-673 (1975).

Howe, M.S., "The Influence of surface rounding on trailing edge noise," J Sound Vib.126(3), 503-523 (1988).

Howe, M.S., "Structural and acoustic noise generated by a large-eddy break-up device," Proc Roy Soc Lond. A424,461-486 (1989).

Howe, M.S. Acoustics of Fluid-Structure Interactions, 1st ed., Cambridge University Press, (1998a).

Howe, M.S. "Reference Manual on the theory of lifting surface noise at low Mach numbers," Boston Univ. Report AM-98-001 (1998b).

Howe, M. 'Trailing Edge Noise at Low Mach Numbers," JSV, 225(2), 211-238 (1999).

Howe, M. "Trailing Edge Noise at Low Mach Numbers, Part 2: Attached and Separated Edge Flows," JSV 234(5), 761-775 (2000).

Howe,M.S., "Edge-Source Acoustic Green's function for an airfoil of arbitrary chord, with application to trailing–edge noise," Q. J. Mech. Appl. Math. 54(1), 139-155 (2001a).

Howe, M.S., "Unsteady Lift and Sound Produced by An Airfoil in a Turbulent Boundary Layer," J Fluids and Structures 15, 207-225 (2001b).

Kraichnan,R.H., "Pressure fluctuations in Turbulent Flow Over a Flat Plate," J. Acoustical Society of America, Vol. 28,No. 3, pp.378-390, (1956).

Landahl, M.J., Unsteady Transonic Flow, New York: Pergamon Press (1961).

Lighthill, M.J., Introduction to Fourier Analysis and Generalised Functions, Cambridge University Press (1958).

Martinez, R. and Widnall, S.E., " Unified Aerodynamic-Acoustic Theory for a Thin Rectangular wing encountering a Gust," AIAA Journal, Vol. 18, June 1980, pp.636-645 (1980).

Martinez, R. and Rudzinsky, J. "Analytic Evaluation of Shape effects on blade-vortex interaction," CAA Report U-2466-402.14 (Dec. 1997).

Meecham, W. C., "Surface and Volume Sound from Boundary Layers," JASA 37(3), 516-522 (1965).

Moon, L.F., and Zelazny, S.W., "Experimental and "Analytical Study of Jet Noise Modeling", AIAA J, V. 13,No. 3 (March 1975).

Olsen, W. and Wagner, J. "Effect of Thickness on airfoil Surface Noise,"AIAA 82-4068 (1982).

Paterson, R.W., and Amiet, R.K., "Noise and Surface Pressure Response of an Airfoil to Incident Turbulence," NASA CR-2733 (Sept. 1976).

Paterson, R.W., and Amiet, R.K., "Noise and Surface Pressure Response of an Airfoil to Incident Turbulence," J. Aircraft, V.14, No. 8, 729-736 (1977).

Powell, A. "Aerodynamic Noise and the plane boundary,"J Acoustical Soc.Am, V32, pp. 982-990 (1960).

Roger, M., Moreau, S., and Wang, M., " An analytical model for predicting airfoil self-noise using wall pressure statistics," Center for Turbulence Research Annual Briefs, NASA Ames and Stanford University, pp.405-414 (2002).

Sears,W. R., "Some aspects of non-stationary airfoil theory and its practical applications." J Aeronautical Sci, V.8,104-108 (1941).

Wygnaski, I., and Fieldler, H., "Some measurements in the self-preserving jet," J. Fluid Mechanics, Vol. 38, Part 3, pp.577-612 (1969).

INITIAL DISTRIBUTION (U)

DIVISION DISTRIBUTION

Organization	Code	Name	Code	Name
NAVSEA			503	Jessup
	PEO-SUB-RT1	Stout		
	PEO-SUB-RT2	Meijida	508	Brown
	05H	Crockett	508	Cox
ONR			70	
	ONR 334	Kim		
			7020	Strasberg
DTIC				
			7051	Blake
			7052	Feit
			7053	Liu
			72	Shang
			725	Noll
			725	Farabee
			725	Gershfeld (5 copies)
			725	Gonzales
			725	Goody
			725	Lynch
			725	Maga
			725	Minniti
			725	Roth
			725	Wojno
			725	Zawadzki